10.1098/rspa.2000.0602

THE ROYAL SOCIETY

Phase singularities in isotropic random waves

By M. V. Berry and M. R. Dennis

H. H. Wills Physics Laboratory, University of Bristol, Tyndall Avenue, Bristol BS8 1TL, UK

Received 3 November 1999; accepted 31 January 2000

The singularities of complex scalar waves are their zeros; these are dislocation lines in space, or points in the plane. For waves in space, and waves in the plane (propagating in two dimensions, or sections of waves propagating in three), we calculate some statistics associated with dislocations for isotropically random Gaussian ensembles, that is, superpositions of plane waves equidistributed in direction but with random phases. The statistics are: mean length of dislocation line per unit volume, and the associated mean density of dislocation points in the plane; eccentricity of the ellipse describing the anisotropic squeezing of phase lines close to dislocation cores; distribution of curvature of dislocation lines in space; distribution of transverse speeds of moving dislocations; and position correlations of pairs of dislocations in the plane, with and without their strength (topological charge) ± 1. The statistics depend on the frequency spectrum of the waves. We derive results for general spectra, and specialize to monochromatic waves in space and the plane, and black-body radiation.

Keywords: phase; dislocations; Gaussian; waves; randomness; singularities

1. Introduction

Phase singularities, that is, dislocations of wavefronts (Nye & Berry 1974; Berry 1981, 1998; Nye 1999)—also called optical vortices—are lines in space, or points in the plane, where the phase χ of the complex scalar wave

$$\psi(\boldsymbol{r},t)=\rho(\boldsymbol{r},t)\exp\{\mathrm{i}\chi(\boldsymbol{r},t)\},\quad \boldsymbol{r}=\{x,y,z\},\tag{1.1}$$

is undefined. For the generic smooth ψ we are interested in, dislocations are also loci of vanishing ρ: in light, they are lines of darkness; in sound, threads of silence. Interest in optical dislocations has recently revived, largely as a result of experiments with laser fields (Karman *et al.* 1997; Beijersbergen 1996; Soskin 1997). In low-temperature physics, ψ could represent the complex order parameter associated with quantum flux lines in a superconductor or quantized vortices in a superfluid.

This revival prompts us to re-examine that part of the theory dealing with the statistical aspects of dislocations in random waves. Previous studies of these statistics have been restricted to quasimonochromatic paraxial waves (Berry 1978; Baranova *et al.* 1981) and experiments and theory for monochromatic waves in two dimensions (Freund *et al.* 1993; Freund 1994, 1997; Freund & Shvartsman 1994; Freund & Freilikher 1997; Freund & Wilkinson 1998; Shvartsman & Freund 1994). Here we are able to go further, and calculate analytically statistics describing a variety of geometrical aspects (see § 2) of dislocations that need not be monochromatic and that are as

far as possible from paraxial, namely statistically isotropic. Our results will include statistics of dislocation lines for waves propagating in three dimensions, and dislocation points for waves in the plane, including, in the latter case, waves propagating in two dimensions and also plane sections of waves propagating in space.

The calculations (see § 4) are possible because we employ the model of wave fields as stationary Gaussian random functions (see § 3), that is, superpositions of many plane waves with random phases. Important special cases are monochromatic waves (see § 5) and black-body radiation (see § 6) caricatured by the scalar-wave approximation (employed by Rayleigh 1889; Einstein & Hopf 1910*a*,*b*). Notwithstanding these results, our treatment is incomplete in several important ways, described in § 7. Readers uninterested in the technicalities of the calculations can ignore §§ 3 and 4.

It will be convenient to separate ψ into its real and imaginary parts,

$$\psi(\boldsymbol{r},t)=\xi(\boldsymbol{r},t)+\mathrm{i}\eta(\boldsymbol{r},t). \tag{1.2}$$

Then dislocations are the intersection lines of the two surfaces

$$\xi(\boldsymbol{r},t)=0, \qquad \eta(\boldsymbol{r},t)=0. \tag{1.3}$$

All the dislocation statistics we will calculate are gauge invariant in the sense of being unaltered by any smooth ($\boldsymbol{r}$ and t dependent) redefinition of phase χ, or, equivalently, any smooth rotation in ξ, η space.

For the average of any quantity F over the ensemble of random ψ, we will use the notation $\langle F\rangle$. For waves propagating in two dimensions, and two-dimensional sections of three-dimensional waves, we will use the notation

$$\boldsymbol{R}\equiv\{x,y\}, \tag{1.4}$$

and denote the corresponding gradients by $\nabla_{\boldsymbol{R}}$ and associated planar averages by suffixes 2. We will also use suffixes to denote derivatives,

$$\xi_x\equiv\frac{\partial\xi}{\partial x}, \quad \text{etc.} \tag{1.5}$$

2. Dislocation geometry

The *current* associated with ψ is

$$\boldsymbol{J}=\mathrm{Im}(\psi^*\nabla\psi)=\rho^2\nabla\chi. \tag{2.1}$$

In the following, a central role will be played by the *vorticity* associated with $\boldsymbol{J}$, namely

$$\boldsymbol{\Omega}=\tfrac{1}{2}\nabla\times\boldsymbol{J}=\tfrac{1}{2}\,\mathrm{Im}(\nabla\psi^*\times\nabla\psi)=\nabla\xi\times\nabla\eta. \tag{2.2}$$

The vector $\boldsymbol{\Omega}$ is important because it points along the dislocation line. This is because it is perpendicular to the normals to the two surfaces (1.3). Around the dislocation line, χ increases by 2π in a positive sense with respect to $\boldsymbol{\Omega}$. We will also need the *unit tangent vector* $\boldsymbol{t}$ along the dislocation line,

$$\boldsymbol{t}=\boldsymbol{\Omega}/\omega, \qquad \omega\equiv|\boldsymbol{\Omega}|. \tag{2.3}$$

For dislocation points in the x,y-plane, the *strength* Q (also called topological charge) can be defined (Halperin 1981; Berry 1998) as $+1$ (-1) if χ increases (decreases) by 2π in a positive circuit with respect to $\boldsymbol{e}_z$,

$$Q\equiv\mathrm{sgn}\,\boldsymbol{\Omega}\cdot\boldsymbol{e}_z=\mathrm{sgn}(\xi_x\eta_y-\xi_y\eta_x). \tag{2.4}$$

(Higher strengths can also occur (Nye & Berry 1974), but this is non-generic.)

(*a*) *Dislocation densities*

The magnitude ω is also the Jacobian determinant transforming ξ and η to local coordinates perpendicular to the dislocation, so *the total length of dislocation line* in any volume V is

$$L(V) = \int_V \mathrm{d}\boldsymbol{r}\, \delta\{\xi(\boldsymbol{r})\}\delta\{\eta(\boldsymbol{r})\}\omega(\boldsymbol{r}), \tag{2.5}$$

where here and hereafter $\mathrm{d}\boldsymbol{r} = \mathrm{d}x\,\mathrm{d}y\,\mathrm{d}z$, and we have not written any time dependence explicitly. It follows that the *dislocation line density*, defined as the mean length of dislocation line per unit volume, is

$$d = \langle \delta(\xi)\delta(\eta)\omega\rangle = \langle \delta(\xi)\delta(\eta)|\nabla\xi \times \nabla\eta|\rangle. \tag{2.6}$$

In the plane, the mean number of dislocation lines piercing unit area of a plane is the *dislocation point density* (cf. Berry 1978),

$$d_2 = \langle \delta(\xi)\delta(\eta)|\boldsymbol{\Omega}\cdot\boldsymbol{e}_z|\rangle = \langle \delta(\xi)\delta(\eta)|\xi_x\eta_y - \xi_y\eta_x|\rangle. \tag{2.7}$$

Both d and d_2 have the dimensions $(\text{length})^{-2}$. It will be convenient to define *dislocation averages* of any quantity f in space or in the plane as

$$\langle f\rangle_{\mathrm{d}} \equiv \frac{1}{d}\langle \delta(\xi)\delta(\eta)\omega f\rangle, \qquad \langle f\rangle_{2,\mathrm{d}} \equiv \frac{1}{d}\langle \delta(\xi)\delta(\eta)|\xi_x\eta_y - \xi_y\eta_x|f\rangle. \tag{2.8}$$

These select dislocations with weights given by transverse delta-functions, so that volume integrals give f integrated along the dislocations within the volume, correctly weighted by arc length.

(*b*) *Core structure*

Around a dislocation line, χ changes by 2π, but the change is usually non-uniform (as has been noticed in numerical calculations (Mondragon & Berry 1989)). To understand this *core structure*, note first that, for a dislocation passing through $\boldsymbol{r} = \boldsymbol{0}$, the current and amplitude near the dislocation have the forms

$$\left.\begin{aligned} \boldsymbol{J}(\boldsymbol{r}) &\approx \boldsymbol{\Omega}(0)\times\boldsymbol{r} && \text{for small } r,\\ \rho^2(\boldsymbol{r}) \to |\boldsymbol{r}\cdot\nabla\psi|^2 &\approx (\boldsymbol{r}\cdot\nabla\xi(0))^2 + (\boldsymbol{r}\cdot\nabla\eta(0))^2 && \text{for small } r, \end{aligned}\right\} \tag{2.9}$$

where $r \equiv |\boldsymbol{r}|$. Therefore, the lines of $\boldsymbol{J}$ are circles enclosing the dislocation (hence the alternative term vortices), and the quadratic form for ρ^2 implies that the local contours of amplitude are ellipses. These observations are connected with the variation of phase through (2.1), so

$$\nabla\chi(\boldsymbol{r}) \approx \frac{\boldsymbol{\Omega}(0)\times\boldsymbol{r}}{(\boldsymbol{r}\cdot\nabla\xi(0))^2 + (\boldsymbol{r}\cdot\nabla\eta(0))^2} \quad \text{for small } r. \tag{2.10}$$

Therefore, the polar plot of $\sqrt{|\nabla\chi|}$ around a circle coaxial with the dislocation is an ellipse with the same eccentricity as the ρ contours, namely

$$\varepsilon = \sqrt{1 - \lambda_-/\lambda_+}, \tag{2.11}$$

where $\lambda_\pm$ are the eigenvalues of the quadratic form in (2.9). A short calculation gives

$$\lambda_\pm = \tfrac{1}{2}\big[(\nabla\xi)^2 + (\nabla\eta)^2 \pm \sqrt{[(\nabla\xi)^2 + (\nabla\eta)^2]^2 - 4\omega^2}\big], \tag{2.12}$$

where all quantities are evaluated on the dislocation. Therefore, the eccentricity is

$$\varepsilon = \frac{1}{\sqrt{2}\omega}([(\nabla\xi)^2 + (\nabla\eta)^2]^2 - 4\omega^2)^{1/4}\sqrt{(\nabla\xi)^2 + (\nabla\eta)^2 - \sqrt{[(\nabla\xi)^2 + (\nabla\eta)^2]^2 - 4\omega^2}}. \tag{2.13}$$

We will calculate the spatial and planar *core eccentricity averages*

$$\langle\varepsilon\rangle_{\mathrm{d}} \quad \text{and} \quad \langle\varepsilon\rangle_{2,\mathrm{d}}. \tag{2.14}$$

Freund & Freilikher (1997) calculate two quantities describing the dislocation core structure: the angle between ψ_x and ψ_y, and the ratio $|\psi_x|/|\psi_y|$. Neither is invariant under rotation in the x, y-plane, but taken together they are equivalent to specifying ε and the orientation of the ellipse. In the same paper, a polar plot of $|\nabla\chi|$ is displayed, corresponding to a curve more complicated than the ellipse generated by $\sqrt{|\nabla\chi|}$.

(*c*) *Curvature*

Dislocation lines are usually *curved*. The curvature is (Eisenhart 1960; do Carmo 1976)

$$\kappa(\boldsymbol{r}) = |(\boldsymbol{t}\cdot\nabla\boldsymbol{t})|. \tag{2.15}$$

We will calculate the *probability distribution of the curvature*, which, from (2.3) can be written, after a short calculation, as

$$P(\kappa) = \langle\delta(\kappa - \kappa(\boldsymbol{r}))\rangle_{\mathrm{d}} = \frac{2\kappa}{d}\left\langle \delta(\xi)\delta(\eta)\omega\delta\left\{\kappa^2 - \frac{|\boldsymbol{t}\times(\boldsymbol{t}\cdot\nabla)\boldsymbol{\Omega}|^2}{\omega^2}\right\}\right\rangle. \tag{2.16}$$

(*d*) *Velocity*

In waves that are not monochromatic, dislocation lines *move*. Their transverse velocity $\boldsymbol{v}(\boldsymbol{r}, t)$ (perpendicular to the dislocation lines) is determined by differentiating (1.3), to get

$$\boldsymbol{v}\cdot\nabla\xi = -\xi_t, \qquad \boldsymbol{v}\cdot\nabla\eta = -\eta_t \tag{2.17}$$

and then verifying the solution

$$\boldsymbol{v}(\boldsymbol{r}, t) = \frac{(\xi_t\nabla\eta - \eta_t\nabla\xi)\times\boldsymbol{\Omega}}{\omega^2}. \tag{2.18}$$

In three dimensions and in the plane, we will calculate the probability distribution of $v = |\boldsymbol{v}|$, that is,

$$P(v) = \langle\delta\{v - v(\boldsymbol{r}, t)\}\rangle_{\mathrm{d}} = 2v\langle\delta\{v^2 - v(\boldsymbol{r}, t)^2\}\rangle_{\mathrm{d}}. \tag{2.19}$$

(*e*) *Correlations*

Dislocations are not independent random lines in space; their positions are correlated. The simplest characterization of the correlations is in the plane, where the two simplest non-local statistics can be defined as follows. Let

$$\xi_{\rm A} \equiv \xi(\boldsymbol{R}_{\rm A}), \qquad \xi_{\rm B} \equiv \xi(\boldsymbol{R}_{\rm B}), \qquad \boldsymbol{R}_{\rm B} \equiv \boldsymbol{R}_{\rm A} + \boldsymbol{R}. \tag{2.20}$$

The *pair correlation function* $g(\boldsymbol{R})$ is the mean density of dislocations at position $\boldsymbol{R}_{\rm A} + \boldsymbol{R}$, given that there is a dislocation at $\boldsymbol{R}_{\rm A}$, normalized to unity at $|\boldsymbol{R}| = \infty$, where the dislocations are independent (at least in the statistical model we will use). Thus (cf. equation (2.7))

$$g(\boldsymbol{R}) \equiv \frac{\langle \delta(\xi_{\rm A})\delta(\eta_{\rm A})\delta(\xi_{\rm B})\delta(\eta_{\rm B})|\omega_{\rm A}||\omega_{\rm B}|\rangle}{d_2^2}, \tag{2.21}$$

where now we use the notation

$$\omega_{\rm A} = \xi_{{\rm A}x}\eta_{{\rm A}y} - \xi_{{\rm A}y}\eta_{{\rm A}x}, \qquad \omega_{\rm B} = \xi_{{\rm B}x}\eta_{{\rm B}y} - \xi_{{\rm B}y}\eta_{{\rm B}x}, \tag{2.22}$$

in which the sign of ω is the strength (charge) of the dislocation (cf. equation (2.4)). The pair correlation satisfies $g(\boldsymbol{R}) \to 1$ as $|\boldsymbol{R}| \to \infty$.

Similarly, the *charge correlation function* $g_Q(\boldsymbol{R})$ (Halperin 1981) gives the normalized density of dislocations separated by $\boldsymbol{R}$, but weighted with their strengths so that opposite dislocations contribute negatively, that is, equation (2.21) without the modulus signs,

$$g_Q(\boldsymbol{R}) \equiv \frac{\langle \delta(\xi_{\rm A})\delta(\eta_{\rm A})\delta(\xi_{\rm B})\delta(\eta_{\rm B})\omega_{\rm A}\omega_{\rm B}\rangle}{d_2^2}. \tag{2.23}$$

Later we will show that the integral of the charge over all $\boldsymbol{R}$ must compensate the charge associated with the dislocation at $\boldsymbol{R} = \boldsymbol{0}$, that is,

$$2\pi d_2 \int_0^\infty {\rm d}R\, R g_Q(R) = -1 \tag{2.24}$$

(of course, this implies $g_Q(\boldsymbol{R}) \to 0$ as $|\boldsymbol{R}| \to \infty$). This is a local neutrality condition, known in the theory of ionic liquids as the first Stillinger–Lovett sum rule (Stillinger & Lovett 1968*a*,*b*). For dislocations, it is the 'critical-point screening' discussed by Freund & Wilkinson (1998). Comparison of $\omega_{\rm A}$ and $\omega_{\rm B}$ for small $\boldsymbol{R}$ shows that, at the origin, g_Q and g are related by

$$g(0) = -g_Q(0). \tag{2.25}$$

Two other correlation statistics, defined by analogy with useful quantities in the theory of ionic liquids (Hansen & McDonald 1986), are the pair correlations between dislocations of the same strength, $g_{++}(\boldsymbol{R})$, and with opposite strengths, $g_{+-}(\boldsymbol{R})$. In terms of $g(\boldsymbol{R})$ and $g_Q(\boldsymbol{R})$,

$$g_{++}(\boldsymbol{R}) = g(\boldsymbol{R}) + g_Q(\boldsymbol{R}), \qquad g_{+-}(\boldsymbol{R}) = g(\boldsymbol{R}) - g_Q(\boldsymbol{R}). \tag{2.26}$$

3. Gaussian random waves

We consider an ensemble of superpositions of infinitely many scalar complex non-dispersive plane waves with speed c,

$$\psi(\boldsymbol{r},t)=\sum_{\boldsymbol{k}} a_{\boldsymbol{k}}\exp\{\mathrm{i}[\boldsymbol{k}\cdot\boldsymbol{r}-ckt-\phi_{\boldsymbol{k}}]\}, \tag{3.1}$$

with wavevectors

$$\boldsymbol{k}=\{k_x,k_y,k_z\},\quad k\equiv|\boldsymbol{k}|. \tag{3.2}$$

For waves in the plane, $\boldsymbol{r}$ and $\boldsymbol{k}$ are replaced by $\boldsymbol{R}$ and $\boldsymbol{K}=\{K_x,K_y\}$, with $K=|\boldsymbol{K}|$. Except where otherwise stated, the following holds equally for $\boldsymbol{k}$ and $\boldsymbol{K}$.

The real amplitudes $a_{\boldsymbol{k}}$ are fixed, and specify the spectrum of the waves as will be explained soon. The $\phi_{\boldsymbol{k}}$ are *random phases* parametrizing the ensemble. Ensemble averages are averages over $0\leqslant\phi_{\boldsymbol{k}}\leqslant 2\pi$ for all $\boldsymbol{k}$, but the functions ψ are ergodic, so ensemble averages are equal to spatial or planar averages.

If the $\boldsymbol{k}$ are suitably dense, any linear combination of the real and imaginary parts (1.2) of (3.1) and their $\boldsymbol{r}$ and t derivatives are stationary Gaussian random functions (Goodman 1985; Rice 1944, 1945 (reprinted in Wax 1954)), whose central properties will now be stated for future reference. Consider any set of N functions

$$\boldsymbol{u}(\boldsymbol{r},t)=\{u_1(\boldsymbol{r},t)\dots u_N(\boldsymbol{r},t)\}, \tag{3.3}$$

in which each u_n is ξ or η or any of their derivatives, and any set of auxiliary variables

$$\boldsymbol{b}=\{b_1\dots b_N\}. \tag{3.4}$$

Then

$$\langle\exp\{\mathrm{i}\boldsymbol{b}\cdot\boldsymbol{u}(\boldsymbol{r},t)\}\rangle=\exp\{-\tfrac{1}{2}\langle(\boldsymbol{b}\cdot\boldsymbol{u})^2\rangle\}=\exp\{-\tfrac{1}{2}\boldsymbol{b}\cdot\boldsymbol{M}\cdot\boldsymbol{b}\}, \tag{3.5}$$

where $\boldsymbol{M}$ is the *matrix of correlations*

$$(\boldsymbol{M})_{mn}=\langle u_m u_n\rangle. \tag{3.6}$$

Using (2.5), the *probability density* of $\boldsymbol{u}(\boldsymbol{r},t)$ can easily be found,

$$\begin{aligned}P(\boldsymbol{u})&\equiv\langle\delta\{\boldsymbol{u}-\boldsymbol{u}(\boldsymbol{r},t)\}\rangle\\&=\frac{1}{(2\pi)^N}\int\mathrm{d}\boldsymbol{b}\,\exp\{-\mathrm{i}\boldsymbol{b}\cdot\boldsymbol{u}\}\langle\exp\{\mathrm{i}\boldsymbol{b}\cdot\boldsymbol{u}(\boldsymbol{r},t)\}\rangle\\&=\frac{\exp\{-\frac{1}{2}\boldsymbol{u}\cdot\boldsymbol{M}^{-1}\cdot\boldsymbol{u}\}}{(2\pi)^{N/2}\sqrt{\det\boldsymbol{M}}}.\end{aligned} \tag{3.7}$$

Before using $P(\boldsymbol{u})$ to calculate the geometrical averages of § 2, it is necessary to determine the correlations $\boldsymbol{M}$ (equation (3.6)), involving averages of products of pairs of u_n. Explicit averaging over $\phi_{\boldsymbol{k}}$ in (3.1) shows that all such quadratic averages are of the form

$$\langle f(\boldsymbol{k})\rangle=\frac{1}{2}\sum_{\boldsymbol{k}}a_{\boldsymbol{k}}^2 f(\boldsymbol{k}). \tag{3.8}$$

Now we make the central specification that the randomness of the waves we are considering is *isotropic*, so that $a_{\boldsymbol{k}}$ depends only on the length k, and define the *radial power spectrum* Π by

$$\left.\begin{aligned} \frac{1}{2}\sum_{\boldsymbol{k}} a_{\boldsymbol{k}}^2 f(\boldsymbol{k}) &\equiv \int \mathrm{d}\boldsymbol{k}\, \frac{\Pi(k)}{4\pi k^2} f(\boldsymbol{k}) \qquad \text{(three dimensions)},\\ \frac{1}{2}\sum_{\boldsymbol{K}} a_{\boldsymbol{K}}^2 f(\boldsymbol{K}) &\equiv \int \mathrm{d}\boldsymbol{K}\, \frac{\Pi_2(K)}{2\pi K} f(\boldsymbol{K}) \quad \text{(two dimensions)}. \end{aligned}\right\} \tag{3.9}$$

For plane sections of waves in three dimensions, Π and Π_2 are related by projection in wavevector space,

$$\begin{aligned} \Pi_2(K) &= 2\pi K \int_{-\infty}^{\infty} \mathrm{d}k_z\, \frac{\Pi(\sqrt{k_z^2+K^2})}{4\pi(k_z^2+K^2)}\\ &= K\int_K^{\infty} \mathrm{d}k\, \frac{\Pi(k)}{k\sqrt{k^2-K^2}}. \end{aligned} \tag{3.10}$$

Multiplication of Π by a constant corresponds to rescaling the strength of the wave ψ and leaves all dislocation averages unaffected. It is convenient to normalize Π to unity, that is,

$$\int_0^{\infty} \mathrm{d}k\, \Pi(k) = 1, \qquad \int_0^{\infty} \mathrm{d}K\, \Pi_2(K) = 1, \tag{3.11}$$

so that the fundamental averages are

$$\langle \xi^2 \rangle = \langle \eta^2 \rangle = 1. \tag{3.12}$$

For radial averages and radial moments, it will be convenient to use the notation

$$\int_0^{\infty} \mathrm{d}k\, f(k)\Pi(k) \equiv \langle\langle f \rangle\rangle, \qquad \langle\langle k^m \rangle\rangle \equiv k_m, \tag{3.13}$$

and similarly in the plane, indicated by the subscript 2 and with K replacing k.

The quadratic averages needed to calculate the dislocation statistics of § 2 are of two sorts. First, with α denoting x, y or z, there are products of u_α at the same position and time; of these, the only non-zero products are

$$\left.\begin{aligned} \langle \xi_\alpha^2 \rangle = \langle \eta_\alpha^2 \rangle &= -\langle \xi\xi_{\alpha\alpha} \rangle = -\langle \eta\eta_{\alpha\alpha} \rangle = \tfrac{1}{3}k_2,\\ \langle \xi_\alpha^2 \rangle_2 = \langle \eta_\alpha^2 \rangle_2 &= \tfrac{1}{2}K_2,\\ \langle \xi_{\alpha\alpha}^2 \rangle = \langle \eta_{\alpha\alpha}^2 \rangle &= \tfrac{1}{5}k_4,\\ \langle \xi_{\alpha\beta}^2 \rangle = \langle \eta_{\alpha\beta}^2 \rangle = \langle \xi_{\alpha\alpha}\xi_{\beta\beta} \rangle = \langle \eta_{\alpha\alpha}\eta_{\beta\beta} \rangle &= \tfrac{1}{15}k_4 \quad (\alpha \neq \beta),\\ \langle \xi_t^2 \rangle = \langle \eta_t^2 \rangle &= c^2 k_2,\\ \langle \xi\eta_t \rangle = -\langle \eta\xi_t \rangle &= ck_1. \end{aligned}\right\} \tag{3.14}$$

Second, there are products involving different positions. These occur in the planar correlation statistics (2.21) and (2.23). The fundamental averages of this non-local type are (cf. equation (2.20))

$$C(R) \equiv \langle \xi_{\mathrm{A}}\xi_{\mathrm{B}} \rangle = \langle \eta_{\mathrm{A}}\eta_{\mathrm{B}} \rangle = \langle\langle J_0(KR) \rangle\rangle_2 = \left\langle \left\langle \frac{\sin(kR)}{kR} \right\rangle \right\rangle, \tag{3.15}$$

defining the *autocorrelation function* $C(R)$, and where the last equality applies to plane sections of waves propagating in space. To write the remaining non-zero non-local averages, we can choose the x-axis to lie along the direction of the vector $\boldsymbol{R} = \boldsymbol{R}_{\mathrm{B}} - \boldsymbol{R}_{\mathrm{A}}$. Then

$$\left.\begin{aligned}\langle\xi_{\mathrm{A}}\xi_{\mathrm{B}x}\rangle &= \langle\eta_{\mathrm{A}}\eta_{\mathrm{B}x}\rangle = -\langle\xi_{\mathrm{A}x}\xi_{\mathrm{B}}\rangle \\ &= -\langle\eta_{\mathrm{A}x}\eta_{\mathrm{B}}\rangle = -\langle\langle KJ_1(KR)\rangle\rangle_2 \equiv C'(R), \\ \langle\xi_{\mathrm{A}x}\xi_{\mathrm{B}x}\rangle &= \langle\eta_{\mathrm{A}x}\eta_{\mathrm{B}x}\rangle = -\langle\langle K^2J_0''(KR)\rangle\rangle_2 = -C''(R), \\ \langle\xi_{\mathrm{A}y}\xi_{\mathrm{B}y}\rangle &= \langle\eta_{\mathrm{A}x}\eta_{\mathrm{B}y}\rangle = \frac{1}{R}\langle\langle KJ_1(KR)\rangle\rangle_2 = -\frac{C'(R)}{R}.\end{aligned}\right\} \tag{3.16}$$

All other relevant averages, local and non-local, are zero. Note, in particular, that all averages involving both ξ and η vanish, except $\langle\xi\eta_t\rangle = -\langle\eta\xi_t\rangle$.

Our calculations will be for general radial power spectra Π. However, the following are important special cases. For *monochromatic waves* propagating in space and in the plane, the respective spectra are densities on a spherical shell in $\boldsymbol{k}$ space and on a ring in $\boldsymbol{K}$ space:

$$\Pi(k) = \delta(k - k_0), \qquad \Pi_2(K) = \delta(K - K_0). \tag{3.17}$$

For *plane sections of monochromatic waves in space*, we have, from (3.10), the projection of the sphere spectrum

$$\Pi_2(K) = \frac{K\Theta(k_0 - K)}{k_0\sqrt{k_0^2 - K^2}}, \tag{3.18}$$

where Θ denotes the unit step. For *black-body radiation* with temperature T, and thermal wavenumber defined by

$$k_T \equiv \frac{k_{\mathrm{B}}T}{\hbar c}, \tag{3.19}$$

where k_{B} is Boltzmann's constant, the radial (Planck) spectrum is

$$\Pi(k) = \frac{15k^3}{\pi^4 k_T^4[\exp(k/k_T) - 1]}. \tag{3.20}$$

4. Calculation of averages for general spectra

In calculating averages, we make use of the joint probability density of the magnitude of vorticity ω and the gauge-invariant quantity

$$G \equiv |\nabla\psi|^2 = (\nabla\xi)^2 + (\nabla\eta)^2. \tag{4.1}$$

As shown in Appendix A, the three-dimensional distribution is

$$P(\omega, G) = \frac{27\omega}{2k_2^3}\exp\left\{-\frac{3G}{2k_2}\right\}\Theta(G - 2\omega), \tag{4.2}$$

and, in the plane,

$$P_2(\omega, G) = \frac{2}{K_2^2}\exp\left\{-\frac{G}{K_2}\right\}\Theta(G - 2\omega). \tag{4.3}$$

(*a*) *Dislocation densities*

For the line density (2.6), we note that all quantities in the average are independent, so

$$d = \frac{1}{2\pi}\int_0^\infty \mathrm{d}G \int_0^\infty \mathrm{d}\omega\, \omega P(\omega, G). \tag{4.4}$$

With (4.2), the integral is elementary, and gives

$$d = k_2/3\pi. \tag{4.5}$$

For the point density (2.7), a similar argument based on (4.3) gives

$$d_2 = K_2/4\pi. \tag{4.6}$$

If ψ in the plane is a section of a wave in space, equation (3.10) applies, and gives

$$K_2 = \tfrac{2}{3}k_2, \tag{4.7}$$

whence

$$d_2 = \tfrac{1}{2}d. \tag{4.8}$$

In this result, the $\frac{1}{2}$ is the spherical average of the factor $|\cos\theta|$ relating contributions to d and d_2 from lines making angles θ with the normals to the faces of a unit cube.

(*b*) *Dislocation core structure*

For the core eccentricity, we require the averages (2.14), involving ω^2 and G. In three dimensions, using (2.13), (4.2) and (4.5), and rescaling G,

$$\langle\varepsilon\rangle_\mathrm{d} = \frac{81}{4\sqrt{2}}\int_0^\infty \mathrm{d}G \int_0^{G/2} \mathrm{d}\omega\, \omega \exp\{-\tfrac{3}{2}G\}(G^2-4\omega^2)^{1/4}\sqrt{G-\sqrt{G^2-4\omega^2}}. \tag{4.9}$$

With the substitution $\omega = \frac{1}{2}uG$, the G integral is trivial, and the u integral can also be evaluated, leading to

$$\langle\varepsilon\rangle_\mathrm{d} = \frac{3\pi}{8\sqrt{2}} = 0.8330. \tag{4.10}$$

In the plane, analogous calculations give

$$\langle\varepsilon\rangle_{2,\mathrm{d}} = 2\sqrt{2}\int_0^\infty \mathrm{d}G \int_0^{G/2} \mathrm{d}\omega\, \exp\{-G\}(G^2-4\omega^2)^{1/4}\sqrt{G-\sqrt{G^2-4\omega^2}}, \tag{4.11}$$

leading to

$$\langle\varepsilon\rangle_{2,\mathrm{d}} = \frac{3}{\sqrt{2}}\sinh^{-1}1 - 1 = 0.8697. \tag{4.12}$$

These eccentricities are rather large (figure 1), showing that the typical phase structure is strongly anisotropic. Note that the eccentricities are independent of the spectra Π and Π_2; they are universal numbers characterizing the dislocation cores of isotropic random waves in space and the plane. It is not surprising that the planar eccentricity is greater than for three dimensions, where the amplitude contours are elliptic cylinders surrounding the dislocations, because plane sections slice these cylinders obliquely.

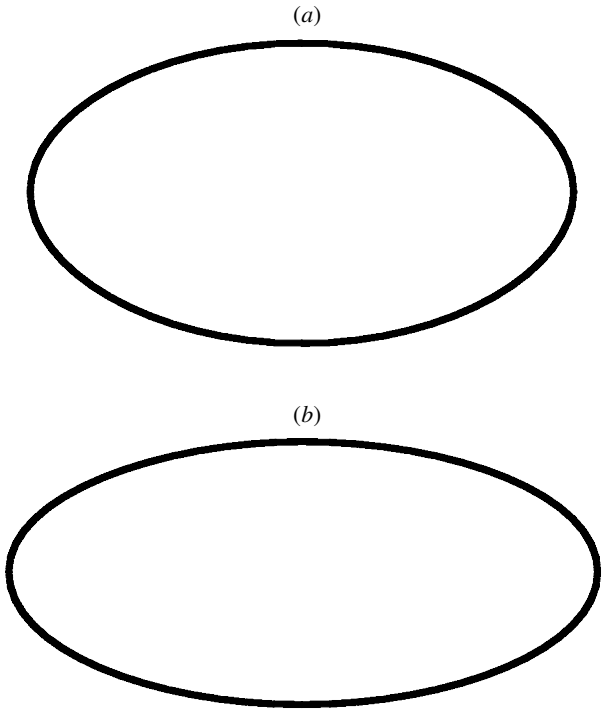

Figure 1. Ellipses representing anisotropy of phase structure near dislocation cores. (a) Transverse to dislocations in space. (b) In the plane.

(c) *Dislocation curvature*

For the curvature (2.16), calculations are greatly simplified by evaluating the derivatives of $\boldsymbol{\Omega}$ in local coordinates whose z-axis is along $\boldsymbol{\Omega}$. Then

$$\begin{aligned}\kappa(\boldsymbol{r})^2 &= \frac{(\partial_z\Omega_x)^2+(\partial_z\Omega_y)^2}{\omega^2}\\ &= \frac{1}{\omega^2}(\xi_{zz}^2(\nabla\eta)^2+\eta_{zz}^2(\nabla\xi)^2-2\xi_{zz}\eta_{zz}\nabla\xi\cdot\nabla\eta).\end{aligned} \tag{4.13}$$

The only non-diagonal correlation matrix (cf. equations (3.3) and (3.6)) is

$$M=\begin{pmatrix}1 & -\frac{1}{3}k_2\\ -\frac{1}{3}k_2 & \frac{1}{5}k_4\end{pmatrix}\quad\text{for } \boldsymbol{u}=\{\xi,\xi_{zz}\}, \tag{4.14}$$

whence

$$P(\xi=0,\xi_{zz})=\frac{1}{2\pi\kappa_{\mathrm{c}}\sqrt{k_2}}\exp\left\{-\frac{\xi_{zz}^2}{2\kappa_{\mathrm{c}}^2k_2}\right\}, \tag{4.15}$$

where κ_{c} is the *characteristic curvature*

$$\kappa_{\mathrm{c}}\equiv\sqrt{\frac{9k_4-5k_2^2}{45k_2}}. \tag{4.16}$$

From (2.16), we need to calculate the dislocation average

$$P(\kappa) = \frac{\kappa}{\pi}\int_{-\infty}^{\infty} \mathrm{d}q\, \exp\{-\mathrm{i}q\kappa^2\}\langle \exp\{\mathrm{i}q\kappa(\boldsymbol{r})^2\}\rangle_{\mathrm{d}}, \tag{4.17}$$

where κ^2 is given by (4.13). The averages over ξ_{zz} and η_{zz} now involve a two-dimensional complex Gaussian integral. In evaluating this, and also the trivial averages over ξ and η, it is convenient to transform to the scaled curvature

$$\kappa_{\mathrm{sc}} \equiv \frac{\kappa}{\kappa_{\mathrm{c}}}, \qquad P(\kappa) = \frac{1}{\kappa_{\mathrm{c}}}P(\kappa_{\mathrm{sc}}), \tag{4.18}$$

and also to rescale ω and G. Then we find, after substituting for d from (4.5),

$$P(\kappa_{\mathrm{sc}}) = \frac{3\kappa_{\mathrm{sc}}}{2\pi}\int_{-\infty}^{\infty} \mathrm{d}q\, \exp\{-\mathrm{i}q\kappa_{\mathrm{sc}}^2\}\left\langle \frac{\omega}{\sqrt{D(\omega,G,q)}}\right\rangle, \tag{4.19}$$

where D, the determinant from the Gaussian integration, is

$$D(\omega,G,q) = 1 - 2\mathrm{i}\frac{qG}{\omega^2} - 4\frac{q^2}{\omega^2}. \tag{4.20}$$

Some non-obvious manipulations are required to apply (4.2) to the evaluation of the triple integral in (4.19) (over q, ω and G). These are explained in Appendix B.

The result is

$$P(\kappa_{\mathrm{sc}}) = \frac{3^{5/2}\kappa_{\mathrm{sc}}}{(\kappa_{\mathrm{sc}}^2+3)^{5/2}}. \tag{4.21}$$

All moments diverge except the first two, which are

$$\langle\kappa\rangle_{\mathrm{d}} = \sqrt{3}\kappa_{\mathrm{c}}, \qquad \langle\kappa^2\rangle_{\mathrm{d}} = 6\kappa_{\mathrm{c}}^2. \tag{4.22}$$

(*d*) *Dislocation speed*

We use (2.18) and (2.19); the squared speed is

$$v(\boldsymbol{r},t)^2 = \frac{1}{\omega^2}[\xi_t^2(\nabla\eta)^2 + \eta_t^2(\nabla\xi)^2 - 2\xi_t\eta_t\nabla\xi\cdot\nabla\eta]. \tag{4.23}$$

The only non-diagonal correlation matrices are

$$\mathsf{M}_{\pm} = \begin{pmatrix} 1 & \pm ck_1 \\ \pm ck_1 & c^2k_2 \end{pmatrix} \quad \text{for } \boldsymbol{u}_+ = \{\xi,\eta_t\}, \quad \boldsymbol{u}_- = \{\eta,\xi_t\}, \tag{4.24}$$

whence

$$P(\xi=0,\eta_t) = \frac{1}{2\pi v_{\mathrm{c}}\sqrt{k_2}}\exp\left\{-\frac{\eta_2^2}{2v_{\mathrm{c}}^2k_2}\right\} \tag{4.25}$$

(and similarly for η, ξ_t), where v_{c} is the *characteristic speed*

$$v_{\mathrm{c}} \equiv c\sqrt{(1-k_1^2/k_2)}. \tag{4.26}$$

This is for three dimensions; for waves propagating in the plane, k_1 and k_2 must be replaced by K_1 and K_2, and we denote the characteristic speed by v_{c2}.

The complete formal similarity between (4.23), (4.25) and (4.13)–(4.15) in the curvature calculation means that the speed distribution in three dimensions can be written by analogy with (4.21), after rescaling to the dimensionless speed

$$v_{sc} \equiv \frac{v}{v_c}, \qquad P(v) = \frac{1}{v_c} P(v_{sc}). \tag{4.27}$$

The distribution is

$$P(v_{sc}) = \frac{3^{5/2} v_{sc}}{(v_{sc}^2 + 3)^{5/2}}. \tag{4.28}$$

All moments diverge except the first two, which are

$$\langle v \rangle_d = \sqrt{3} v_c, \qquad \langle v^2 \rangle_d = 6 v_c^2. \tag{4.29}$$

In the plane, the analogous result, obtained with the aid of (4.3) rather than (4.2), is

$$P_2(v_{sc}) = \frac{4 v_{sc}}{(v_{sc}^2 + 2)^2}. \tag{4.30}$$

Only the first moment does not diverge,

$$\langle v \rangle_{d,2} = \frac{\pi}{\sqrt{2}} v_{c2}. \tag{4.31}$$

As written, equations (4.30) and (4.31) apply to waves propagating in the plane. For plane sections of waves propagating in space, v_{c2} must be replaced by the three-dimensional v_c of (4.26) (because, for such sections, $\omega = ck$, not cK).

It is important to note that the speeds v in the spatial and planar distributions (4.28) and (4.30) can take any value from zero to infinity: v is not limited by the common speed c of the dispersionless waves in the superposition (3.1). This is not a violation of relativity, because dislocations are forms rather than things (like searchlight beams and intersections of scissor blades): no energy moves with them (because they are zeros) and they cannot be used to transmit information. In fact, it is possible to construct simple exact solutions of the dispersionless wave equation possessing single dislocations moving with arbitrary speed (Nye & Berry 1974).

(*e*) *Dislocation correlations*

For the pair correlation (2.21), we eliminate the modulus signs using the identity

$$|\omega| = \frac{1}{\pi} \int_{-\infty}^{\infty} \frac{\mathrm{d}t}{t^2} (1 - \cos(\omega t)). \tag{4.32}$$

Thus (2.21) becomes

$$g(R) = \frac{1}{d_2^2 \pi^2} \int_{-\infty}^{\infty} \frac{\mathrm{d}t_A}{t_A^2} \int_{-\infty}^{\infty} \frac{\mathrm{d}t_B}{t_B^2} [T(0,0) - T(t_A,0) - T(t_B,0) + \tfrac{1}{2}(T(t_A,t_B) + T(t_A,-t_B))], \tag{4.33}$$

where

$$T(t_{\rm A},t_{\rm B})=\langle\delta(\xi_{\rm A})\delta(\eta_{\rm A})\delta(\xi_{\rm B})\delta(\eta_{\rm B})\exp\{{\rm i}(\omega_{\rm A}t_{\rm A}-\omega_{\rm B}t_{\rm B})\}\rangle. \tag{4.34}$$

The merit of this substitution is that since the ω depend quadratically on ξ and η, the average in (4.34) will involve only a Gaussian integral.

There are two non-diagonal correlation matrices, since, from (3.16), the two vectors

$$\boldsymbol{u}_1=\{\xi_{\rm A},\xi_{\rm B},\xi_{{\rm A}x},\xi_{{\rm B}x}\},\qquad \boldsymbol{u}_2=\{\xi_{{\rm A}y},\xi_{{\rm B}y}\} \tag{4.35}$$

are independent (and similarly for correlations involving η). With the notations

$$\left.\begin{aligned} &C\equiv C(R),\\ &E\equiv C'(R),\\ &H\equiv -C'(R)/R,\\ &F\equiv -C''(R),\\ &F_0\equiv -C''(0)=\tfrac{1}{2}K_2,\end{aligned}\right\} \tag{4.36}$$

the matrices corresponding to $\boldsymbol{u}_1$ and $\boldsymbol{u}_2$ are

$$\mathsf{M}_1=\begin{pmatrix}1 & C & 0 & E\\ C & 1 & -E & 0\\ 0 & -E & F_0 & F\\ E & 0 & F & F_0\end{pmatrix},\qquad \mathsf{M}_2=\begin{pmatrix}F_0 & H\\ H & F_0\end{pmatrix}. \tag{4.37}$$

We need

$$\left.\begin{aligned} &\det\mathsf{M}_1\equiv D_1=[E^2-(1+C)(F_0-F)][E^2-(1-C)(F_0+F)],\\ &\det\mathsf{M}_2\equiv D_2=F_0^2-H^2.\end{aligned}\right\} \tag{4.38}$$

Then the relevant probability densities are

$$\left.\begin{aligned} P(\xi_{\rm A}=0,\xi_{\rm B}=0,\xi_{{\rm A}x},\xi_{{\rm B}x})&=\frac{\exp\{-\frac{1}{2}\boldsymbol{u}_1'\cdot\mathsf{N}_1\cdot\boldsymbol{u}_1'\}}{(2\pi)^2D_1},\\ P(\xi_{{\rm A}y},\xi_{{\rm B}y})&=\frac{\exp\{-\frac{1}{2}\boldsymbol{u}_2\cdot\mathsf{N}_2\cdot\boldsymbol{u}_2\}}{(2\pi)^2D_2},\end{aligned}\right\} \tag{4.39}$$

where

$$\left.\begin{aligned} &\boldsymbol{u}_1'\equiv\{\xi_{{\rm A}x},\xi_{{\rm B}x}\},\\ &\mathsf{N}_1=\frac{1}{D_1}\begin{pmatrix}-[E^2-F_0(1-C^2)] & cE^2-F(1-C^2)\\ cE^2-F(1-C^2) & -[E^2-F_0(1-C^2)]\end{pmatrix},\\ &\mathsf{N}_2=\frac{1}{D_2}\begin{pmatrix}F_0 & -H\\ -H & F_0\end{pmatrix},\end{aligned}\right\} \tag{4.40}$$

and similarly for η.

The average (4.35) is now an eight-dimensional complex Gaussian integral whose evaluation gives

$$T(t_{\rm A},t_{\rm B})=\frac{1}{(2\pi)^2D(t_{\rm A},t_{\rm B})}, \tag{4.41}$$

where

$$D(t_{\rm A},t_{\rm B}) = (1-C^2)^2 + (t_{\rm A}^2+t_{\rm B}^2)F_0(E^2-F_0(1-C^2)) \\ - t_{\rm A}t_{\rm B}H(CE^2-F(1-C^2)) + t_{\rm A}^2t_{\rm B}^2D_1D_2. \quad (4.42)$$

Now, after scaling $t_{\rm A}$ and $t_{\rm B}$, the pair correlation (4.33) becomes

$$g(R) = \frac{F_0(E^2-F_0(1-C^2))}{4\pi^4 d_2^2(1-C^2)^2}\int_{-\infty}^{\infty}\frac{{\rm d}t_{\rm A}}{t_{\rm A}^2}\int_{-\infty}^{\infty}\frac{{\rm d}t_{\rm B}}{t_{\rm B}^2}I(t_{\rm A},t_{\rm B},Y,Z), \quad (4.43)$$

where

$$Y \equiv \frac{H^2(CE^2-F(1-C^2))^2}{F_0^2(E^2-F_0(1-C^2))^2}, \qquad Z \equiv \frac{D_1D_2(1-C^2)}{F_0^2(E^2-F_0(1-C^2))^2} \quad (4.44)$$

and

$$I(t_{\rm A},t_{\rm B},Y,Z) = 1-\frac{1}{1+t_{\rm A}^2}-\frac{1}{1+t_{\rm B}^2}+\frac{1+t_{\rm A}^2+t_{\rm B}^2+Zt_{\rm A}^2t_{\rm B}^2}{(1+t_{\rm A}^2+t_{\rm B}^2+Zt_{\rm A}^2t_{\rm B}^2)^2-4Yt_{\rm A}^2t_{\rm B}^2}. \quad (4.45)$$

Because I is a rational function, the $t_{\rm A}$ integral can be evaluated by residues, leaving, after integrating by parts over $t_{\rm B}$ and substituting for d_2 from (4.6), the pair correlation

$$g(R) = \frac{2(E^2-F_0(1-C^2))}{\pi F_0(1-C^2)^2}\int_0^{\infty}{\rm d}t\,\frac{3-Z+2Y+(3+Z-2Y)t^2+2Zt^4}{(1+t^2)^3\sqrt{1+(1+Z-Y)t^2+Zt^4}}. \quad (4.46)$$

It is possible to express this as an explicit, but very complicated, combination of elliptic integrals, that we do not write. In any case, the integral converges very well and is easy to evaluate numerically.

For the charge correlation (2.23), the absence of modulus signs makes the evaluation much easier, since the average can be expressed as derivatives of Gaussian integrals involving the probability densities (4.39). The result, expressed using the notation (4.36), is

$$g_Q(R) = \frac{2E(CE^2-F(1-C^2))}{RF_0^2(1-C^2)^2} = \frac{1}{F_0^2R}\partial_R\left(\frac{E^2(R)}{1-C^2(R)}\right). \quad (4.47)$$

The first equality is a special case of a formula previously obtained by Halperin (1981). The second equality, together with $E(0)=0$, leads immediately to the screening relation (2.24).

We can get further insight into critical-point screening by considering the charge $Q(N)$ associated with the dislocations within an area $A = N/d_2$, where the mean number of dislocations is N ($N \gg 1$). Obviously, the average charge $\langle Q(N)\rangle$ is zero. But what about the mean square fluctuation $\langle Q^2(N)\rangle$? If the charges merely have average neutrality, there are no long-range correlations, and we expect $\langle Q^2(N)\rangle \sim N$. An exact calculation (with the boundary of A Gauss-smoothed to eliminate trivial edge effects) gives (for all N)

$$\langle Q^2(N)\rangle = \tfrac{1}{2}N\left(1+2\pi d_2\int_0^{\infty}{\rm d}R\,Rg_Q(R)\exp\left\{\frac{\pi R^2}{2A}\right\}\right) \\ = \tfrac{1}{2}N\left(1+2\pi d_2\int_0^{\infty}{\rm d}R\,Rg_Q(R)\right) + \tfrac{1}{2}d_2^2\pi^2\int_0^{\infty}{\rm d}R\,R^3g_Q(R) + O(N^{-1}). \quad (4.48)$$

Without critical-point screening, the leading term is the first one, and the fluctuations are those of a random distribution with overall neutrality. But for dislocations, there is screening, and the first term vanishes, leaving fluctuations that are *independent of* N for large N. Further manipulation gives

$$\langle Q^2(A)\rangle = \frac{1}{8}\int_0^\infty \mathrm{d}R\, R^2 \partial_R\left[\frac{C'(R)^2}{1-C^2(R)}\right] + O(N^{-1}). \tag{4.49}$$

5. Monochromatic waves

For *monochromatic waves in space* with wavenumber $k_0 = 2\pi/\lambda$, the spectrum is (3.17), and so the dislocation line density (4.5) is

$$d = \frac{k_0^2}{3\pi}. \tag{5.1}$$

For a plane section of the same wave, the density (4.6) of dislocation points is

$$d_2 = \frac{k_0^2}{6\pi} = \frac{2\pi}{3\lambda^2}. \tag{5.2}$$

A measure of the spacing of these points is

$$\frac{1}{\sqrt{d_2}} = 0.691\lambda. \tag{5.3}$$

The characteristic curvature (4.16) is $\kappa_\mathrm{c} = 2k_0/\sqrt{45}$, so the curvature averages (4.22) are

$$\langle\kappa^2\rangle_\mathrm{d} = 2\langle\kappa\rangle_\mathrm{d}^2 = \tfrac{8}{15}k_0^2. \tag{5.4}$$

A measure of the radius of curvature is

$$1/\sqrt{\langle\kappa^2\rangle} = 0.218\lambda, \tag{5.5}$$

indicating that dislocations are rather sharply curved on the wavelength scale.

For the pair and charge correlation statistics $g(R)$ and $g_Q(R)$, we need the autocorrelation function (3.15),

$$C(R) = \frac{\sin(k_0 R)}{k_0 R}. \tag{5.6}$$

Figure 2 shows $g(R)$ and $g_Q(R)$, calculated from (4.46) and (4.47). At the origin, $g(0) = -g_Q(0) = \frac{2}{5}$, showing modest repulsion between dislocations.

For monochromatic waves in the plane, with wavenumber $K_0 = 2\pi/\Lambda$ with ring spectrum (3.17), the density of dislocation points is

$$d_2 = \frac{K_0^2}{4\pi} = \frac{\pi}{\Lambda^2}. \tag{5.7}$$

A measure of the spacing of these points is

$$1/\sqrt{d_2} = 0.564\Lambda. \tag{5.8}$$

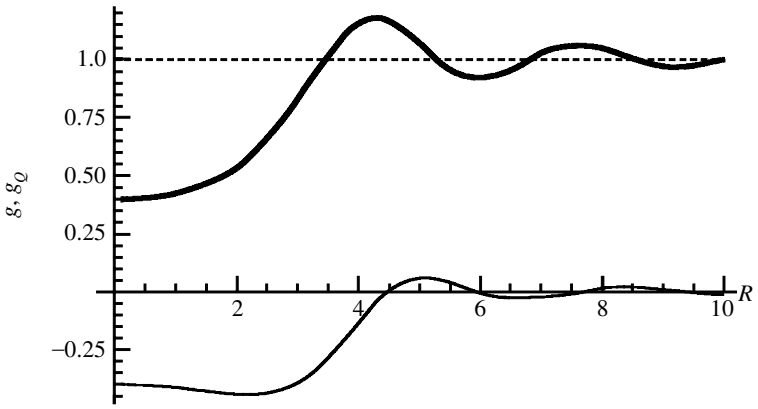

Figure 2. Correlation statistics for a plane section of monochromatic waves in space, in units of k_0. Thick line: pair correlation $g(R)$. Dashed line: asymptotic value $g = 1$. Thin line: charge correlation $g_Q(R)$.

The autocorrelation function (3.15) is

$$C(R) = J_0(K_0 R), \tag{5.9}$$

from which the pair and charge correlations can be calculated (figure 3). At the origin, $g(0) = -g_Q(0) = 1/4$, indicating a stronger repulsion between dislocations. Note that, except very close to the origin, there is no obvious relation between g and g_Q. Now, the strength Q (equation (2.4)) alternates between neighbouring dislocations on the net formed by the intersections of zero lines of ξ and η; this is the 'sign principle' (Freund & Shvartsman 1994). Thus one might expect that alternate maxima of g ('rings' of dislocations) would correspond to maxima and minima of g_Q (representing oppositely charged rings of dislocations). But the topological relation seems not to have a metrical counterpart. We have checked this by calculating g and g_Q for a 'blurred' square lattice, of alternating dislocations whose vertices are randomly displaced according to a Gaussian distribution; if the blurring becomes comparable with the lattice spacing, there is again no relation between g and g_Q. The only vestige of the sign principle in the charge correlations (Shvartsman & Freund 1994) seems to be the fact that $g_Q(0)$ is negative (cf. equation (2.25)).

Of course, for monochromatic waves the dislocations do not move.

6. Black-body radiation

With the spectrum (3.20), involving the thermal wavenumber (3.19), the wavenumber moments (3.13) are

$$\left.\begin{aligned} k_n &= \frac{15}{\pi^4} k_T^n (n+3)!\zeta(n+4), \\ k_1 &= 3.832 k_T, \\ k_2 &= \tfrac{40}{21}\pi^2 k_T^2, \\ k_4 &= 8\pi^4 k_T^4, \end{aligned}\right\} \tag{6.1}$$

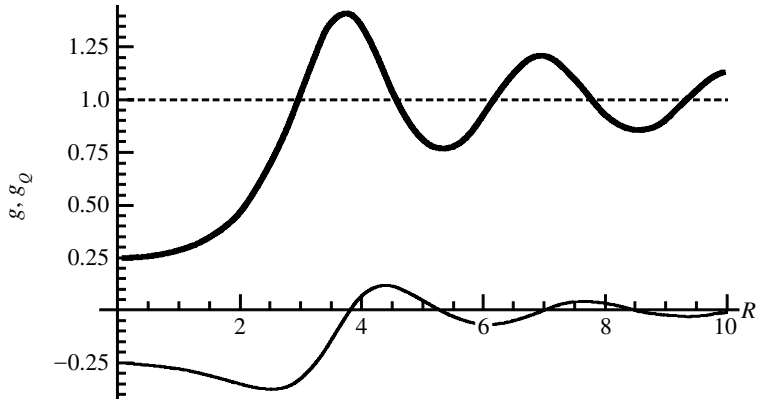

Figure 3. Correlation statistics for monochromatic waves in the plane, in units of K_0. Thick line: pair correlation $g(R)$. Dashed line: asymptotic value $g = 1$. Thin line: charge correlation $g_Q(R)$.

so the dislocation line density (4.5) is

$$d = \tfrac{40}{63}\pi k_T^2. \tag{6.2}$$

For a plane section of the same wave, the density (4.6) of dislocation points is

$$d_2 = \tfrac{20}{63}\pi k_T^2 = \frac{80\pi^3}{63\lambda_T^2}, \tag{6.3}$$

where $\lambda_T = 2\pi/kT$ is the thermal wavelength. A measure of the spacing of these points is

$$1/\sqrt{d_2} = 0.159\lambda_T. \tag{6.4}$$

This seems rather small, but it should be noted that λ_T does not correspond to the maximum of the Planck k-distribution (3.20); this lies at $k = 2.831k_T$, corresponding to a wavelength $0.354\lambda_T$.

The curvature statistics (4.22) are

$$\langle\kappa^2\rangle_{\mathrm{d}} = 2\langle\kappa\rangle_{\mathrm{d}}^2 = \tfrac{5938}{1575}k_T^2. \tag{6.5}$$

A measure of the radius of curvature is

$$1/\sqrt{\langle\kappa^2\rangle} = 0.026\lambda_T, \tag{6.6}$$

indicating that (even though λ_T is not the maximum of the Planck distribution) dislocations are even more sharply curved than in the monochromatic case (5.5), showing the effect of large wavenumbers in the Planck distribution.

For the characteristic speed (4.26), equations (6.1) give $v_{\mathrm{c}} = 0.468c$, whence the moments (4.29) of the transverse speed are

$$\sqrt{\langle v_{\mathrm{d}}^2\rangle} = \sqrt{2}\langle v\rangle_{\mathrm{d}} = 1.146c. \tag{6.7}$$

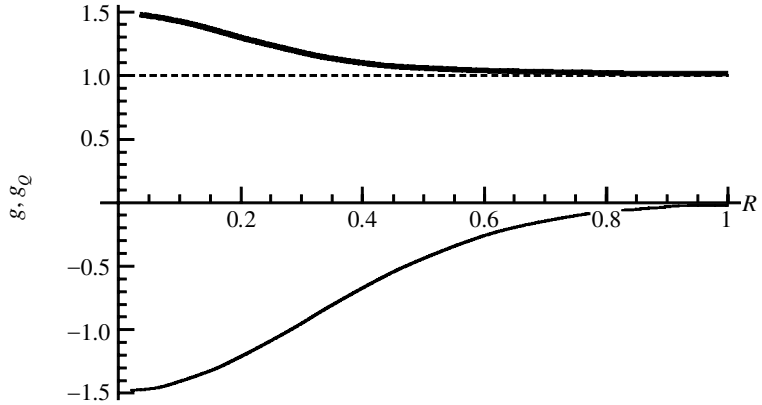

Figure 4. Correlation statistics for a plane section of black-body radiation, in units of the thermal wavenumber k_T. Thick line: pair correlation $g(R)$. Dashed line: asymptotic value $g = 1$. Thin line: charge correlation $g_Q(R)$.

For the pair and charge correlation statistics $g(R)$ and $g_Q(R)$, we need the autocorrelation function (3.15). This can be calculated as

$$C(R) = \frac{30}{\pi^4}\sum_{n=1}^{\infty}\frac{3n^2-(k_TR)^2}{[n^2+(k_TR)^2]^3} = \frac{30}{\pi^4}\left[\frac{1}{(k_TR)^2}-\pi^2\frac{k_TR\cosh(k_TR)}{\sinh^2(k_TR)}\right]. \tag{6.8}$$

Figure 4 shows $g(R)$ and $g_Q(R)$, calculated from (4.46) and (4.47). At the origin, $g(0) = -g_Q(0) = 3/2$, showing considerable clustering (anti-repulsion) between dislocations, notwithstanding the topological sign repulsion.

7. Concluding remarks

We have calculated some statistics that describe the geometry of dislocation lines in complex scalar Gaussian random waves in two and three dimensions. In this, the wave equation played only a minor role—restricting the time dependence of the plane-wave constituents, and so affecting the calculations of speed. Apart from this, the results apply to any complex scalar random functions, not just the waves that are our main interest.

The geometry thus revealed is extraordinarily complicated and occasionally counterintuitive: dislocations sharply curved on the wavelength scale, moving faster than light, and with positions correlated in ways apparently unrelated to the topological alternation of sign. Nevertheless, much remains to be understood, both mathematically and physically.

For local statistics, a fully three-dimensional characterization requires understanding of the *torsion* as well as the curvature. Preliminary investigation suggests that the mean-square torsion diverges and the distribution of torsion has a long tail, indicating that dislocations are typically locally helical rather than flat rings. For non-local statistics, the correlations g and g_Q are just the start of an infinite hierarchy of N-dislocation correlations, and there are also position correlations between the speeds

of dislocations. More interesting are global, that is, topological, statistics. We can ask: are dislocation lines typically closed in space? Can they be knotted? If knotted, what is the distribution of knot invariants (Adams 1994)? Since (as it is easy to show by example) pairs of dislocations can be linked, what is the distribution of linking numbers? If higher-order links are possible (e.g. Borromean triples (Cromwell *et al.* 1998)), what is the distribution of numbers characterizing such links?

Finally, we mention the application to black-body radiation. Given the importance of black-body radiation in physics, it is a little surprising that its detailed geometric structure has not been fully understood. Here we have made some progress, but as a physical model, the scalar-wave approximation is inadequate. Better would be an understanding of the singularities of the electromagnetic field of black-body radiation, but it is not clear what the relevant singularities are—the vector singularities studied so far (Nye 1983*a*,*b*, 1999; Nye & Hajnal 1987) are restricted either to paraxial or monochromatic waves, and so are inapplicable here. We are studying this question now.

We are grateful to Dr John Hannay for many helpful suggestions and to Professor Isaac Freund for a useful correspondence. M.V.B.'s research is supported by The Royal Society; in addition, he thanks the Lorentz Institute of the University of Leiden for generous hospitality while writing the first draft of this paper. M.R.D. is supported by a University of Bristol postgraduate scholarship.

Appendix A. Joint probability distribution of $\boldsymbol{\omega}$ and G

Defining the 3-vectors $\boldsymbol{a} = \nabla\xi$, $\boldsymbol{b} = \nabla\eta$ and $a = |\boldsymbol{a}|$, $b = |\boldsymbol{b}|$, we have, from (2.2), (2.3) and (4.1),

$$P(\omega, G) = \langle \delta(\omega - |\boldsymbol{a} \times \boldsymbol{b}|)\delta(G - a^2 - b^2)\rangle. \tag{A 1}$$

All components of $\boldsymbol{a}$ and $\boldsymbol{b}$ are independent, so the matrix of correlations is diagonal and, using (3.14) and polar coordinates for $\boldsymbol{a}$ and $\boldsymbol{b}$, with the z-axis for $\boldsymbol{b}$ along $\boldsymbol{a}$,

$$P(\omega, G) = \frac{27}{\pi k_2^3} \int_0^\infty \mathrm{d}a\, a^2 \int_0^\infty \mathrm{d}b\, b^2 \int_0^\pi \mathrm{d}\theta\, \sin\theta \times \exp\left\{-\frac{3(a^2+b^2)}{2k_2}\right\} \delta(\omega - ab\sin\theta)\delta(G - a^2 - b^2). \tag{A 2}$$

With the successive changes of variable

$$a = \rho\cos\phi, \qquad b = \rho\sin\phi, \qquad \phi = \tfrac{1}{2}\gamma, \qquad \sin\theta\sin\gamma = s, \qquad \sin\gamma = t, \tag{A 3}$$

evaluation is straightforward though tedious, and gives (4.2).

The planar calculation, in which $\boldsymbol{a}$ and $\boldsymbol{b}$ are 2-vectors, proceeds similarly, and gives (4.3).

Appendix B. Curvature and speed integrals

We outline the calculation for curvature in three dimensions; for speed in three dimensions, the calculation is identical, and for speed in the plane the arguments are very similar. With (4.2), equation (4.19) becomes

$$P(\kappa_{\mathrm{sc}}) = \frac{81\kappa_{\mathrm{sc}}}{4\pi} \int_{-\infty}^\infty \mathrm{d}q\, \exp\{-\mathrm{i}q\kappa_{\mathrm{sc}}^2\} \int_0^\infty \mathrm{d}G\, \exp\{-\tfrac{3}{2}G\} \int_0^{G/2} \mathrm{d}\omega\, \frac{\omega^2}{\sqrt{D(\omega, G, q)}}. \tag{B 1}$$

Changing to variables

$$\omega = \tfrac{1}{2}G\mu, \qquad q = G\rho \tag{B 2}$$

eliminates G from D and enables the G integral to be evaluated, to give

$$P(\kappa_{\rm sc}) = \frac{243\kappa_{\rm sc}}{4\pi}\int_0^1 {\rm d}\mu\,\mu^3\int_{-\infty}^{\infty}{\rm d}\rho\,\frac{1}{\sqrt{\mu^2-8{\rm i}\rho-16\rho^2}(\frac{3}{2}+{\rm i}\rho\kappa_{\rm sc}^2)^5}. \tag{B 3}$$

The ρ integrand contains a pole and two branch points, which can be connected by a cut. The contour can be deformed around the cut without passing through the pole, and then the further transformations

$$\rho = \tfrac{1}{4}{\rm i}(v-1), \qquad \mu = \sqrt{u} \tag{B 4}$$

lead to

$$P(\kappa_{\rm sc}) = \frac{15\,552\kappa_{\rm sc}}{\pi}\int_0^1 {\rm d}u\,u\int_{-1}^1 {\rm d}v\,\frac{1}{\sqrt{1-v^2}(6+\kappa_{\rm sc}^2-\kappa_{\rm sc}^2 v\sqrt{1-u})^5}. \tag{B 5}$$

Use of

$$\int_{-1}^1\frac{{\rm d}v}{\sqrt{1-v^2}(a+v)^5} = \frac{\pi(3+24a^2+8a^4)}{8(a^2-1)^{9/2}} \tag{B 6}$$

leads to a u integral that is elementary, leading eventually to (4.21).

References

Adams, C. C. 1994 *The knot book*. San Francisco, CA: Freeman.

Baranova, N. B., Zel'dovich, B. Y., Mamaev, A. V., Pilipetskii, N. & Shkukov, V. V. 1981 Dislocations of the wavefront of a speckle-inhomogeneous field (theory and experiment). *JETP Lett.* **33**, 195–199.

Beijersbergen, M. 1996 Phase singularities in optical beams. Thesis, Huygens Laboratory, Leiden.

Berry, M. V. 1978 Disruption of wavefronts: statistics of dislocations in incoherent Gaussian random waves. *J. Phys.* A **11**, 27–37.

Berry, M. V. 1981 Singularities in Waves and Rays. In *Les Houches lecture series* (ed. R. Balian, M. Kléman & J.-P.Poirier), vol. 35, pp. 453–543. Amsterdam: North-Holland.

Berry, M. V. 1998 Much ado about nothing: optical dislocation lines (phase singularities, zeros, vortices, ...). In *Proc. Int. Conf. on Singular Optics* (ed. M. S. Soskin), SPIE vol. 3487, pp. 1–15.

Cromwell, P., Beltrami, E. & Rampicini, M. 1998 The Borromean rings. *Mathematical Intelligencer* **20**, 53–62.

do Carmo, M. P. 1976 *Differential geometry of curves and surfaces*. Englewood Cliffs, NJ: Prentice-Hall.

Einstein, A. & Hopf, L. 1910*a* On a theorem of the probability calculus and its application to the theory of radiation. *Ann. Phys.* **33**, 1096–1104.

Einstein, A. & Hopf, L. 1910*b* Statistical investigation of a resonator's motion in a radiation field. *Ann. Phys.* **33**, 1105–1115.

Eisenhart, L. P. 1960 *A treatise on the differential geometry of curves and surfaces*. New York: Dover.

Freund, I. 1994 Optical vortices in Gaussian random wave-fields—statistical probability densities. *J. Opt. Soc. Am.* A **11**, 1644–1652.

Freund, I. 1997 Critical-point level crossing geometry in random wave fields. *J. Opt. Soc. Am.* **14**, 1911–1927.

Freund, I. & Freilikher, V. 1997 Parameterization of anisotropic vortices. *J. Opt. Soc. Am.* A **14**, 1902–1910.

Freund, I. & Shvartsman, N. 1994 Wave-field phase singularities: the sign principle. *Phys. Rev.* A **50**, 5164–5172.

Freund, I. & Wilkinson, M. 1998 Critical-point screening in random wave fields. *J. Opt. Soc. Am.* A **15**, 2892–2902.

Freund, I., Shvartsman, N. & Frehlikher, V. 1993 Optical dislocation networks in highly random media. *Opt. Commun.* **101**, 247–264.

Goodman, J. W. 1985 *Statistical optics*. Wiley.

Halperin, B. I. 1981 Statistical mechanics of topological defects. In *Les Houches lecture series* (ed. R. Balian, M. Kléman & J.-P. Poirier), vol. 35, pp. 813–857. Amsterdam: North-Holland.

Hansen, J.-P. & McDonald, I. R. 1986 *Theory of simple liquids*. Academic.

Karman, G. P., Beijersbergen, M. W., van Duijl, A. & Woerdman, J. P. 1997 Creation and annihilation of phase singularities in a focal field. *Optics Lett.* **22**, 1503–1505.

Mondragon, R. J. & Berry, M. V. 1989 The quantum phase 2-form near degeneracies: two numerical studies. *Proc. R. Soc. Lond.* A **424**, 263–278.

Nye, J. F. 1983*a* Lines of circular polarization in electromagnetic wave fields. *Proc. R. Soc. Lond.* A **389**, 279–290.

Nye, J. F. 1983*b* Polarization effects in the diffraction of electromagnetic waves: the role of disclinations. *Proc. R. Soc. Lond.* A **387**, 105–132.

Nye, J. F. 1999 *Natural focusing and fine structure of light: caustics and wave dislocations*. Bristol: Institute of Physics Publishing.

Nye, J. F. & Berry, M. V. 1974 Dislocations in wave trains. *Proc. R. Soc. Lond.* A **336**, 165–190.

Nye, J. F. & Hajnal, J. V. 1987 The wave structure of monochromatic electromagnetic radiation. *Proc. R. Soc. Lond.* A **409**, 21–36.

Rayleigh, Lord 1889 On the character of the complete radiation at a given temperature. *Phil. Mag.* **27**, 460–469.

Rice, S. O. 1944 Mathematical analysis of random noise. *Bell. Syst. Tech. J.* **23**, 282–332.

Rice, S. O. 1945 Mathematical analysis of random noise. *Bell. Syst. Tech. J.* **24**, 46–156.

Shvartsman, N. & Freund, I. 1994 Wavefield phase singularities: near-neighbour correlations and anticorrelations. *J. Opt. Soc. Am.* A **11** 2710–2718.

Soskin, M. S. (ed.) 1997 *Proc. Int. Conf. on Singular Optics*, SPIE, vol. 3487.

Stillinger, F. H. & Lovett, R. 1968*a* Ion-pair theory of concentrated electrolytes. I. Basic concepts. *J. Chem. Phys.* **48**, 3858–3868.

Stillinger, F. H. & Lovett, R. 1968*b* General restriction on the distribution of ions in electrolytes. *J. Chem. Phys.* **49**, 1991–1994.

Wax, N. (ed.) 1954 *Selected papers on noise and stochastic processes*. New York: Dover.

Phase singularities in isotropic random waves

By M. V. Berry and M. R. Dennis

Proc. R. Soc. Lond. A **456**, 2059–2079 (2000)

Corrigendum 1. Equation (4.48) and the material to the end of § 3 should be replaced by

$$\begin{aligned}\langle Q^2(N)\rangle &= \tfrac{1}{2}N\left(1+2\pi d_2\int_0^\infty \mathrm{d}R\,Rg_Q(R)\exp\left\{-\frac{\pi R^2}{2A}\right\}\right)\\ &= \frac{1}{4}\int_0^\infty \mathrm{d}R\,R\frac{C'(R)^2}{(1-C(R)^2)}\exp\left(-\frac{\pi R^2}{2A}\right),\end{aligned} \tag{4.48}$$

where in deriving the second equality we have used equation (4.47) and the critical-point screening relation (2.24) that follows from it. The first equality shows that without critical-point screening, the leading term for large N would be $\frac{1}{2}N$, and the fluctuations would be those of a random distribution with overall neutrality. But for dislocations there is screening, and

$$\langle Q^2(N)\rangle = \frac{1}{4}\int_0^\infty \mathrm{d}R\,R\left[\frac{C'(R)^2}{1-C^2(R)}\right]+O(N^{-1}), \tag{4.49}$$

provided the integral converges, leaving fluctuations that are *independent of* N for large N. However, for the sharp spectra representing monochromatic waves in space ((3.17) and (5.6) later), and in the plane ((3.18) and (5.9) later), the integral does not converge. Then we can show from (4.48) that $\langle Q^2(N)\rangle \sim \log N$ for waves in space, and $\langle Q^2(N)\rangle \sim \sqrt{N}$ for waves in the plane.

Corrigendum 2. Equation (6.8) should be replaced by

$$\begin{aligned}C(R) &= \frac{30}{\pi^4}\sum_{n=1}^\infty \frac{3n^2-(k_TR)^2}{[n^2+(k_TR)^2]^3}\\ &= \frac{15}{(\pi k_TR)^4}\left[1-(\pi k_TR)^3\frac{\cosh(\pi k_TR)}{\sinh^3(\pi k_TR)}\right].\end{aligned} \tag{6.8}$$